

# The scenario of two families of compact stars

## 1. Equations of state, mass-radius relations and binary systems

Alessandro Drago<sup>1</sup>, Andrea Lavagno<sup>2</sup>, Giuseppe Pagliara<sup>1</sup>, and Daniele Pigato<sup>2</sup>

<sup>1</sup> Dip. di Fisica e Scienze della Terra dell'Università di Ferrara and INFN Sez. di Ferrara, Via Saragat 1, I-44100 Ferrara, Italy

<sup>2</sup> Department of Applied Science and Technology, Politecnico di Torino and INFN, Sez. di Torino, I-10129 Torino, Italy

Received: date / Revised version: date

**Abstract.** We present several arguments which favor the scenario of two coexisting families of compact stars: hadronic stars and quark stars. Besides the well known hyperon puzzle of the physics of compact stars, a similar puzzle exists also when considering delta resonances. We show that these particles appear at densities close to twice saturation density and must be therefore included in the calculations of the hadronic equation of state. Such an early appearance is strictly related to the value of the  $L$  parameter of the symmetry energy that has been found, in recent phenomenological studies, to lie in the range  $40 < L < 62$  MeV. We discuss also the threshold for the formation of deltas and hyperons for hot and lepton rich hadronic matter. Similarly to the case of hyperons, also delta resonances cause a softening of the equation of state which makes it difficult to obtain massive hadronic stars. Quark stars, on the other hand, can reach masses up to  $2.75M_{\odot}$  as predicted by perturbative QCD calculations. We then discuss the observational constraints on the masses and the radii of compact stars. The tension between the precise measurements of high masses and the indications of the existence of very compact stellar objects (with radii of the order of 10 km) is relieved when assuming that very massive compact stars are quark stars and very compact stars are hadronic stars. Finally, we discuss recent interesting measurements of the eccentricities of the orbits of millisecond pulsars in low mass X-ray binaries. The high values of the eccentricities found in some cases could be explained by assuming that the hadronic star, initially present in the binary system, converts to a quark star due to the increase of its central density.

**PACS.** PACS-key describing text of that key – PACS-key describing text of that key

## 1 Introduction

Ultra-relativistic heavy ions experiments have provided many indications of the formation of a new phase of strongly interacting matter, named quark gluon plasma, which is obtained by heating up hadronic matter (with almost vanishing baryon density) to temperatures of few hundreds MeV [1]. In this state, the fundamental degrees of freedom of QCD, quarks and gluons, are deconfined. A very interesting question of nuclear and hadronic physics concerns the possibility of the formation of a deconfined phase also at large baryon densities and small temperatures. Natural systems to look for this state of matter are neutron stars. In this respect, the recent discoveries of two stellar objects [2,3] with masses of  $M = 2M_{\odot}$  are very promising: the larger the mass the larger the baryon density in the core of the stars. Those massive compact stars are therefore the best systems for studying the structure of the QCD phase diagram at high densities.

There is huge collection of theoretical and phenomenological calculations aiming at establishing whether quark

matter can form in these stellar objects and which would be the possible associated observational signatures. One can distinguish three possible scenarios: i) there is only one family of compact stars which are hybrid stars i.e. stars composed by hadronic matter at low density and quark matter at high density. See for instance Refs. [4,5,6,7] for recent calculations providing equations of state stiff enough to support a star of  $2M_{\odot}$ . ii) high mass “twin compact stars” [8]. In this scenario most of the stars would be composed only of nucleonic matter. Stellar configurations with masses of about  $2M_{\odot}$  could be composed either of nucleonic or of hybrid matter. The two coexisting stellar configurations have different radii: hybrid stars are more compact than their “twin hadronic stars”. iii) two separated families of compact stars [9]: hadronic stars which can be very compact and have a maximum mass of about  $1.5 - 1.6M_{\odot}$ ; quark stars which can be very massive, up to  $2.75M_{\odot}$ , and have large radii.

The third scenario is the one we will present in this paper and in the accompanying paper 2. We will discuss in particular the phenomenological motivations in favor of this model and we will try to analyze the predictions which distinguish this model from the other two. The paper is

*Send offprint requests to:*

organized as follows: in Sec.2 we present the calculations of the equations of state of hadronic and quark matter. In Sec.3 we compare our theoretical results with the observational constraints on the masses and the radii of compact stars. In Sec. 4 we discuss the information one can obtain on the Equation of State (EoS) from the study of compact stars in binary systems. Final discussions and conclusions are presented in Sec. 5.

## 2 Equations of state

In this Section we present the EoS for hadronic and quark matter used in the present investigation. For hadronic matter a problem hugely discussed in the literature concerns how to reconcile the unavoidable appearance of hyperons (at densities of the order of  $2 - 3n_0$ ) with the existence of compact stars with masses of  $2M_\odot$ . This problem is discussed in the contribution of Chatterjee and Vidana in this volume. The similar problem of the appearance of delta resonances at finite density is much less discussed in the literature for reasons that we will clarify in the following. Here we summarize our findings concerning the simultaneous formation of hyperons and deltas within a relativistic mean field approach.

In the first subsection, the  $\beta$ -stable hadronic EoS is studied in the regime of zero temperature within a nonlinear relativistic Walecka-type model and in the framework of the so-called SFHo parametrization which takes into account the recent experimental constraints. In the second subsection, we extend the study of the SFHo model at finite value of entropy per baryon.

### 2.1 Hadronic equations of state including $\Delta$ -isobars and hyperons at $T = 0$

Concerning the hadronic EoS we consider in this paper two different relativistic EoS with the inclusion of the octet of lightest baryons (nucleons and hyperons) and  $\Delta(1232)$  isobar resonances. First, we study the nonlinear GM3 model of Glendenning-Moszkowsky in which the interaction between baryons is mediated by the exchange of a scalar meson  $\sigma$ , an isoscalar vector meson  $\omega$  and a isovector vector  $\rho$  [10]. Let us note that, within the GM3 parametrization, only the experimental value of the symmetry energy at saturation  $S$  is used to fix the coupling between the  $\rho$  meson and the nucleons. However, recently, a remarkable concordance among experimental, theoretical, and observational studies has been found [11], by allowing to significantly constrain also the value of  $L$ , the derivative with respect to the density of the symmetry energy  $S$  at saturation:

$$L = 3n_B \frac{dS}{dn_B} \Big|_{n_B=n_0} . \quad (1)$$

Therefore, extensions of the GM relativistic mean-field model have been implemented which include  $\rho$  meson self-interaction terms. These new parametrization modify the

density dependence of the symmetry energy at supranuclear densities and satisfy all of the experimental constraints both from terrestrial and astrophysical data by restricting  $L$  to the range of  $40 \text{ MeV} \lesssim L \lesssim 62 \text{ MeV}$  [11]. To this purpose, we are going to compare the results in the framework of the GM3 model (with a value of  $L \simeq 80 \text{ MeV}$ , automatically fixed once a specific value of  $S$  is adopted) with a more sophisticated EoS, called SFHo, for which  $S = 32 \text{ MeV}$  (very close to the GM3 value) and  $L = 47 \text{ MeV}$  [12,13].

In the GM3 model the general form of lagrangian is given by [10]

$$\begin{aligned} \mathcal{L}_{\text{octet}} = & \sum_k \bar{\Psi}_k (i\gamma_\mu \partial^\mu - m_k + g_{\sigma k} \sigma - g_{\omega k} \gamma_\mu \omega^\mu - \\ & g_{\rho k} \gamma_\mu \frac{\boldsymbol{\tau}_k}{2} \cdot \boldsymbol{\rho}^\mu) \Psi_k + \frac{1}{2} (\partial_\mu \sigma \partial^\mu \sigma - m_\sigma^2 \sigma^2) \\ & - \frac{1}{4} \omega_{\mu\nu} \omega^{\mu\nu} + \frac{1}{2} m_\omega^2 \omega_\mu \omega^\mu - \frac{1}{4} \rho_{\mu\nu} \cdot \boldsymbol{\rho}^{\mu\nu} \\ & + \frac{1}{2} m_\rho^2 \boldsymbol{\rho}_\mu \cdot \boldsymbol{\rho}^\mu + U(\sigma, \omega, \boldsymbol{\rho}), \end{aligned} \quad (2)$$

where the index  $k$  runs over the baryon octet,  $m_k$  is the bare mass of the baryon  $k$ ,  $\boldsymbol{\tau}_k$  is the isospin operator and finally  $U$  is the mesons potential which can contain non linear interaction terms.

Concerning hyperons, with the exception of the  $\Lambda$ , their binding energies in hypernuclei are highly uncertain (see, for example, Ref. [14] and references therein) and thus also their couplings with mesons are poorly constrained. Here, we use the parameters set of Refs. [15, 16,9] obtained by reproducing the following values of the binding energies in nuclear matter  $U_i^N$ :

$$U_\Lambda^N = -28 \text{ MeV}, U_\Sigma^N = 30 \text{ MeV}, U_\Xi^N = -18 \text{ MeV}. \quad (3)$$

For the coupling with vector mesons we use the SU(6) symmetry relations:

$$\frac{1}{3} g_{\omega N} = \frac{1}{2} g_{\omega \Lambda} = \frac{1}{2} g_{\omega \Sigma} = g_{\omega \Xi} \quad (4)$$

$$g_{\rho N} = \frac{1}{2} g_{\rho \Sigma} = g_{\rho \Xi}, \quad g_{\rho \Lambda} = 0. \quad (5)$$

In relativistic heavy ion collisions, where large values of temperature and density can be reached, a state of resonance matter may be formed and the  $\Delta(1232)$ -isobars are expected to play a central role. [17,18,19,20,21]. Moreover, it has been pointed out that the existence of  $\Delta$ s can be very relevant also in the core of neutron stars [22,23, 24,25,26].

The mean-field Lagrangian density for the  $\Delta$ -isobars can be then expressed as

$$\begin{aligned} \mathcal{L}_\Delta = & \bar{\psi}_{\Delta\nu} [i\gamma_\mu \partial^\mu - (m_\Delta - g_{\sigma\Delta} \sigma) - g_{\omega\Delta} \gamma_\mu \omega^\mu \\ & - g_{\rho\Delta} \gamma_\mu I_3 \boldsymbol{\rho}_3^\mu] \psi_\Delta^\nu, \end{aligned} \quad (6)$$

where  $\psi_\Delta^\nu$  is the Rarita-Schwinger spinor for the  $\Delta$ -isobars ( $\Delta^{++}$ ,  $\Delta^+$ ,  $\Delta^0$ ,  $\Delta^-$ ) and  $I_3 = \text{diag}(3/2, 1/2, -1/2, -3/2)$  is the matrix containing the isospin charges of the  $\Delta$ s.

As customary, for the couplings of hyperons and  $\Delta$  isobars with the mesons, we introduce the ratios

$$x_{\sigma i} = g_{\sigma i}/g_{\sigma N}, \quad x_{\omega i} = g_{\omega i}/g_{\omega N}, \quad x_{\rho i} = g_{\rho i}/g_{\rho N}, \quad (7)$$

where the index  $i$  runs over all the hyperons and  $\Delta$  isobars.

Concerning the values of the  $\Delta$ -meson couplings, if the SU(6) symmetry is exact, one adopts the universal couplings  $x_{\sigma\Delta} = x_{\omega\Delta} = 1$ . As already extensively discussed in Ref. [27], among the four  $\Delta$  isobars, the  $\Delta^-$  is likely to appear first because it can replace a neutron and an electron at the top of their Fermi seas in  $\beta$ -stable matter. However, this particle is “isospin unfavored” because its isospin charge  $t_3 = -3/2$  has the same sign of the isospin charge of the neutron. For large values of the symmetry energy  $S$  and, therefore, of  $g_{\rho\Delta}$ , the  $\Delta^-$  appears at very large densities or it does not appear at all in dense matter thus playing no role in compact stars. Indeed, in Ref. [27] the  $\Delta$ -isobars could appear in neutron stars only for not physical small values of the symmetry energy, obtained by setting  $g_{\rho i} = 0$  for all the baryons. However, as already observed, in the GM3 model the coupling  $g_{\rho N}$  is fixed by using the experimental value of the symmetry energy, the most recent estimates ranging in the interval  $29 \lesssim S \lesssim 32.7$  MeV [11]. In this scheme no experimental information on the density dependence of the symmetry energy can be incorporated and in particular the  $L$  parameter is automatically fixed once a specific value of  $S$  is adopted. It turns out that in the models introduced in Refs. [10,27],  $L \sim 80$  MeV and it is thus significantly higher than the values suggested by the most recent analysis [11].

Moreover, in this context let us observe that the SU(6) symmetry is not exactly fulfilled and one may assume the scalar coupling ratio  $x_{\sigma\Delta} > 1$  with a value close to the mass ratio of the  $\Delta$  and the nucleon [28]. On the other hand, QCD finite-density sum rule results show that the Lorentz vector self-energy for the  $\Delta$  is significantly smaller than the nucleon vector self-energy implying therefore  $x_{\omega\Delta} < 1$  [29].

In the many body analysis of Ref.[30], the real part of the  $\Delta$  self-energy has been evaluated to be about  $-30$  MeV at  $n_B = 0.75 n_0$ . Notice that this self energy is relative to the one of the nucleon and the total potential felt by the  $\Delta$  is the sum of its self energy and of the nucleon potential, a number of the order of  $-80$  MeV. Also phenomenological analysis have been performed of data from electron-nucleus [31,32,33], photo-absorption [34] and pion-nucleus scattering [35,36]. Such analyses suggest a more attractive interaction of the  $\Delta$  in the nuclear medium with respect to the nucleon one (see Refs. [37,38] for more details). New analysis, and possibly new experiments, aiming at a better determinations of these couplings would be extremely important. Notice also that no information is available for  $x_{\rho\Delta}$  which in principle could be extracted by analyzing scattering on neutron rich nuclei (see the recent discussion in [39,40]).

The threshold for the formation of the  $i$ -th baryon is given by the following relation:

$$\mu_i \geq m_i - g_{\sigma i}\sigma + g_{\omega i}\omega + t_{3i}g_{\rho i}\rho, \quad (8)$$

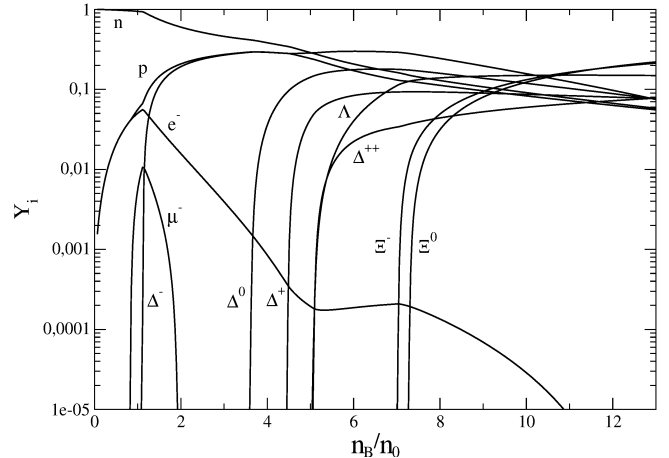


**Fig. 1.** Particles fractions as functions of baryon density (in units of the nuclear saturation density  $n_0$ ) in the GM3 model for  $x_{\sigma\Delta} = 1.25$ ,  $x_{\omega\Delta} = 1$ .

where  $\sigma$ ,  $\omega$  and  $\rho$  are the expectation values of the corresponding fields,  $\mu_i$ ,  $m_i$  and  $t_{3i}$  are the chemical potential, the mass and the isospin charge of the baryons. The baryon chemical potential  $\mu_i$  are obtained by the  $\beta$ -equilibrium conditions:

$$\mu_i = \mu_B + c_i \mu_C, \quad (9)$$

where  $\mu_B$  and  $\mu_C$  are the chemical potentials associated with the conservation of the baryon number and the electric charge respectively and  $c_i$  is the electric charge of the  $i$ -th baryon.

In Fig. 1, we display the baryon density dependence of the particle’s fractions in the GM3 model for  $x_{\sigma\Delta} = 1.25$ ,  $x_{\omega\Delta} = 1$  and neglecting in this case the coupling of the  $\Delta$ -isobars with the  $\rho$  meson ( $x_{\rho\Delta} = 0$ ). Let us note that in this scheme the appearance of the  $\Delta$ -isobars is a consequence of the introduction of a more attractive interaction ( $x_{\sigma\Delta} > 1$ ) of  $\Delta$ -particles with respect to the nucleon in the mean field approximation, as in Refs. [28, 29,41]. It is remarkable that the early appearance of  $\Delta$  resonances, the first one being the  $\Delta^-$ , considerably shifts the onset of hyperons which start to form at densities of  $\sim 5 \rho_0$  (see the curve for the  $\Lambda$ ’s).

At the scope to include the new experimental constraints about the value of the density derivative of the symmetry energy  $L$ , we can first study an extended GM3 model by considering the following density dependent baryon- $\rho$  meson coupling [37,42]

$$g_{\rho i} = g_{\rho i}(n_0)e^{-a(n_B/n_0-1)}. \quad (10)$$

In this way we introduce a single parameter  $a$  which affects only the value of  $L$  leaving untouched the other properties of nuclear matter at saturation.

The role of such density dependent baryon- $\rho$  meson coupling in the modified GM3 model can be observed in Fig. 2, where is reported the value of  $n_{\text{crit}}^B$  for the different baryons as a function of  $L$ . We limit this first discussion

to the case of the  $\Lambda$ ,  $\Delta^-$  and  $\Xi^-$  which are the first heavy baryons appearing as the density increases (notice that  $\Sigma$  hyperons are disfavored due to their repulsive potential) in the so-called universal coupling  $x_{\sigma\Delta} = x_{\omega\Delta} = x_{\rho\Delta} = 1$ . One can notice the different behavior of the thresholds: the larger the value of  $L$  the larger  $n_{\text{crit}}^{\Delta}$  and the smaller  $n_{\text{crit}}^{\Lambda}$  and  $n_{\text{crit}}^{\Xi^-}$ .

At high values of  $L$ , larger than about 65 MeV, the threshold of the  $\Delta^-$  increases very rapidly with  $L$ . This corresponds to the values of  $L$  for which the  $\Xi^-$  appears before the  $\Delta^-$  thus completely suppressing those particles. Indeed within the GM3 model, for which  $L \sim 80$  MeV, the  $\Delta^-$  do not appear at all as already found in Ref. [27]. Similarly, one can notice that if the isobars are formed before the hyperons, what happens below  $L \sim 56$  MeV,  $n_{\text{crit}}^{\Lambda}$  and  $n_{\text{crit}}^{\Xi^-}$  are shifted to larger densities, as already noticed in Ref. [9]. Analogous results have been found in Ref. [27], where two cases are analyzed, corresponding to a finite and to a vanishing value of  $g_{\rho N}$ , with the result that in the case of  $g_{\rho N} = 0$  the isobars are favored. The blue lines mark the range of the values of  $L$  indicated by the analysis of Ref. [11]. Therefore, the recent constraints on  $L$  imply that at densities close to three times  $n_0$  both the hyperons and the isobars must be included in the equation of state and for the lower allowed values of  $L$ , the isobars appear even before the hyperons. Finally, let us stress that in this analysis we have chosen a rather conservative choice for the couplings between  $\Delta$ s and mesons. If higher values of  $x_{\sigma\Delta}$  and or lower values for  $x_{\omega\Delta}$  are adopted,  $n_{\text{crit}}^{\Delta}$  can result to be smaller than  $n_{\text{crit}}^{\Lambda}$  and  $n_{\text{crit}}^{\Xi^-}$  for all the acceptable values of  $L$ .

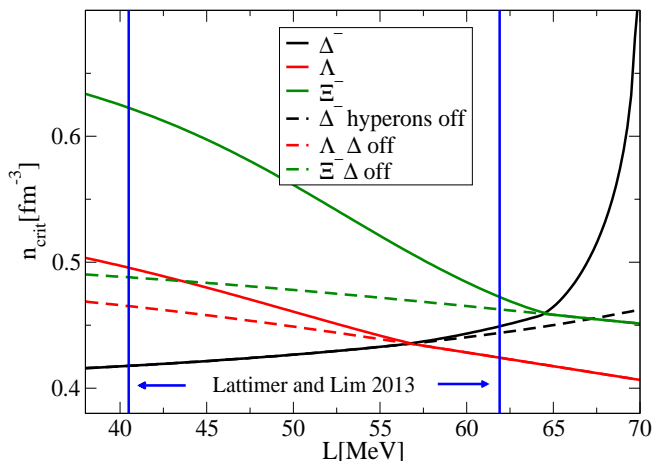


**Fig. 2.** Threshold densities of hyperons and  $\Delta$ s as functions of the  $L$  parameter for  $x_{\sigma\Delta} = x_{\omega\Delta} = x_{\rho\Delta} = 1$  within the modified GM3 model with the introduction of a density dependent baryon- $\rho$  meson coupling (see the text for details). The continuous lines refer to the case in which all the degrees of freedom are included in the computation of the EoS and the dashed lines refer to the case in which either hyperons or  $\Delta$ s are artificially switched off. The vertical lines indicate the range of allowed values of  $L$ , as found in [11].

In comparison with the previous results, we consider now a more sophisticated model for the EoS proposed in Ref. [12,13], where we use the parametrization called SFHo for which  $S = 32$  MeV (very close to the GM3 value) and  $L = 47$  MeV with the addition of hyperons (assuming SU(6) symmetry) and  $\Delta$ -isobar degrees of freedom (assuming  $x_{\sigma\Delta} = x_{\rho\Delta} = 1$  and different values for  $x_{\omega\Delta}$ ).

Results for the particles' fractions as function of the baryon density in  $\beta$ -stable matter within the SFHo model are displayed in Fig. 3. In the upper panel, we have included only hyperons: the  $\Lambda$  and the  $\Xi^-$  appear at a density of about  $0.5 \text{ fm}^{-3}$  and then the  $\Xi^0$  at a density of about  $1.1 \text{ fm}^{-3}$ . In the lower panel we include also the  $\Delta$  isobars. In agreement with what found from the previous analysis, for small values of  $L$  the  $\Delta$ s appear at densities relevant for neutron stars and actually, in the SFHo model, they appear even before the hyperons with the  $\Delta^-$  formed at a density of about  $0.4 \text{ fm}^{-3}$ . The appearance of these particles delays the appearance of hyperons. It is important to remark that, within the SFHo model, even using more repulsive interaction than nucleons,  $x_{\omega\Delta} = 1.1$ , the  $\Delta^-$  appear before hyperons.

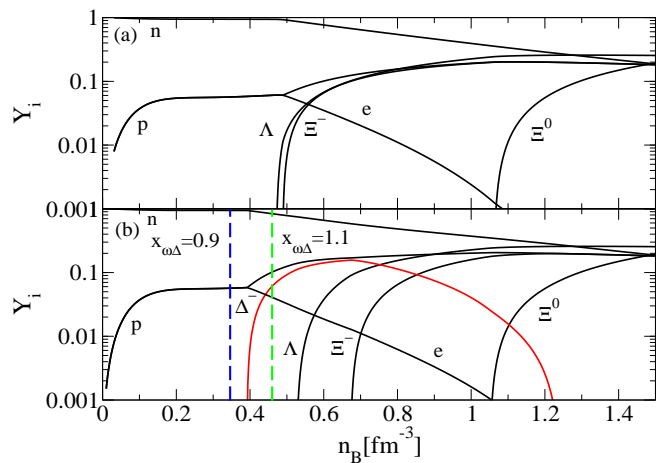


**Fig. 3.** Particles fractions as functions of the baryon density within the SFHo model: only hyperons (panel (a)), hyperons and  $\Delta$ s (panel (b)) for  $x_{\sigma\Delta} = x_{\omega\Delta} = x_{\rho\Delta} = 1$ . The red line indicates the fraction of the  $\Delta^-$  which among the four  $\Delta$ s are the first to appear. The blue and the green vertical lines indicate the onset of the formations of  $\Delta^-$  for  $x_{\omega\Delta} = 0.9$  and  $x_{\omega\Delta} = 1.1$ , respectively.

In conclusion, the early appearance of  $\Delta$ -isobars results to be strictly related to the value of the  $L$  parameter of the symmetry energy and, for physical values of  $L$ , such particle degrees of freedom influence the appearance of hyperons and cannot be neglected in the EoS. These results have been confirmed in the more recent Ref. [43].

## 2.2 Hadronic equation of state at finite entropy per baryon

In this subsection we are going to study the behavior of the hadronic EoS for conditions realized in protonneutron stars (PNS). In particular, we focus our investigation by considering the more realistic SFHo parametrization in the first stage of the protonneutron stars (PNS) evolution, corresponding to a total entropy per baryon equal to one, in which neutrinos are trapped and strongly influence the chemical composition of the PNS. Therefore, we also take into account of leptons particle by fixing the lepton fraction

$$Y_L = Y_e + Y_{\nu_e} = (n_e + n_{\nu_e})/n_B, \quad (11)$$

where  $n_e$ ,  $n_{\nu_e}$  and  $n_B$  are the electron, neutrino and baryon number densities, respectively.

The total entropy per baryon is calculated by means of

$$s = \frac{S_B + S_l}{T \rho_B}, \quad (12)$$

where  $S_B = P_B + \epsilon_B - \sum_{i=B} \mu_i \rho_i$  and  $S_l = P_l + \epsilon_l - \sum_{i=l} \mu_i \rho_i$ , and the sums are extended over all the baryons and leptons species.

It is well known that the presence of trapped neutrinos significantly alter the protons and the electrons abundance and strongly influence the threshold of hyperons formation. This is also true in the presence of  $\Delta$ -isobar degrees of freedom. At the scope of investigating this problem, in Fig. 4, we report the particle concentrations  $Y_i$  as a function of the baryon density for  $s = 1$  and  $Y_L = 0.4$  in the SFHo parametrization with the coupling  $x_{\sigma\Delta} = 1.0$  (upper panel) and  $x_{\sigma\Delta} = 1.1$  (lower panel). In both cases  $x_{\omega\Delta} = x_{\rho\Delta} = 1$ .

Let us observe that, in the case of the universal coupling  $x_{\sigma\Delta} = x_{\omega\Delta} = x_{\rho\Delta} = 1$  (upper panel),  $\Lambda$  and  $\Delta^-$  particles appear approximately at the same baryon density ( $n_B \approx 3n_0$ ). For  $x_{\sigma\Delta} = 1.1$  (lower panel), the onset of  $\Delta^-$  particles is shifted at lower densities and the presence of  $\Delta$ -isobars become more relevant. In both cases, the population of strange  $\Lambda$  particle becomes relevant (greater than 5%) at about  $n_B \approx 4n_0$ .

The features observed in the particle concentration are also reflected in Fig. 5, where we show the temperature as a function of the baryon density for nucleonic matter ( $np$ ), for hyperonic matter ( $npH$ ) and with the inclusion of  $\Delta$ -isobar degrees of freedom ( $npH\Delta$ ). As before, in the presence of  $\Delta$  particles, we have considered two different meson- $\Delta$  couplings (continuous line for  $x_{\sigma\Delta} = 1.0$  and dashed line for  $x_{\sigma\Delta} = 1.1$ ). For  $x_{\sigma\Delta} = 1.0$ ,  $\Lambda$  and  $\Delta^-$  particles start at  $n_B \approx 3n_0$  and, for a large baryon density range, the behavior is almost isothermal ( $T \approx 18 \div 20$  MeV). A more discontinuous behavior can be observed in the case of  $x_{\sigma\Delta} = 1.1$ , due to the presence of the four  $\Delta$ -isobar states.

In Fig. 6, the gravitational mass as a function of the central baryon density  $n_c$  for  $s = 1$  and  $Y_L = 0.4$  is reported for two different values of the  $x_{\sigma\Delta}$  coupling ratio. In this case not appreciable differences can be observed for  $npH$  and  $npH\Delta$  curves (overlapped blue and green curves in the figure), except for a greater central density

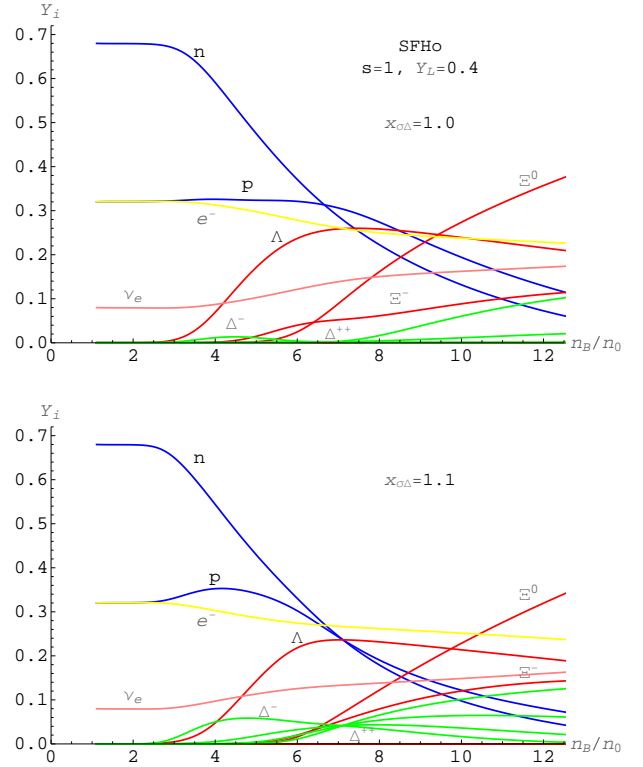


**Fig. 4.** Particle concentrations  $Y_i$  as a function of the baryon density for  $s = 1$  and  $Y_L = 0.4$  in the SFHo parametrization with the coupling  $x_{\sigma\Delta} = 1.0$  (upper panel) and  $x_{\sigma\Delta} = 1.1$  (lower panel). In both cases  $x_{\omega\Delta} = x_{\rho\Delta} = 1$ .

$n_c$  reached in presence of  $\Delta$  particles. In agreement with the previous results, we can see from the figure that hyperons and  $\Delta$ s appear at  $n_B \approx 3n_0$ , corresponding to  $M_G \approx 1.45M_\odot$ . For stellar configurations with masses below this value, deltas and hyperons do not appear or play a marginal role. Therefore we do not expect any difference concerning the SN explosion mechanism in the two families scenario with respect to the standard one. For larger masses there are a few possibilities:

- hyperons appear and trigger the transition to quark matter halting the collapse;
- hyperons appear but their abundance is not large enough to trigger the conversion and a black hole will form after deleptonization [44].

In this little discussion we have not taken into account the rotation of the progenitor what can play an important role as discussed in paper 2.

## 2.3 Quark matter equation of state

The quark matter EoS at densities reachable in the core of compact stars is basically completely unknown. In the

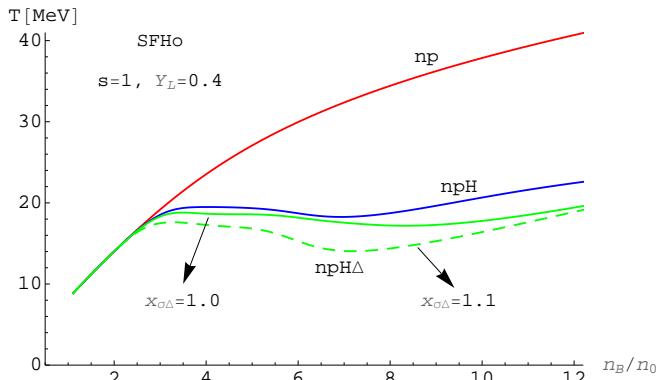


**Fig. 5.** Temperature as a function of the baryon density (in units of  $n_0$ ) at fixed entropy per baryon and lepton fraction ( $s = 1, Y_L = 0.4$ ) for the SFHo parametrization. The labels  $np$ ,  $npH$  and  $npH\Delta$  stand for nucleons, nucleons plus hyperons, nucleons plus hyperons and  $\Delta$ -isobars, respectively. The results for two different meson- $\Delta$  couplings in the curves  $npH\Delta$  are reported, the continuous line refers to  $x_{\sigma\Delta} = 1.0$  while the dashed line stands for  $x_{\sigma\Delta} = 1.1$ .

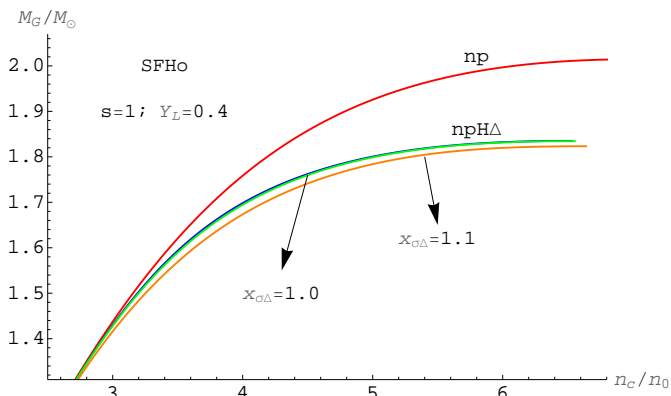


**Fig. 6.** Gravitational mass as a function of the central baryon density  $n_c$  for  $s = 1$  and  $Y_L = 0.4$  in the SFHo parametrization with the couplings  $x_{\sigma\Delta} = 1.0$  and  $x_{\sigma\Delta} = 1.1$ .

literature, bag models or chiral models at finite chemical potential have been widely used which capture two important non-perturbative aspects of QCD: confinement the former and chiral symmetry breaking the latter [45]. Alternatively, one can resort to perturbative QCD calculations: it has been shown that at high temperature, vanishing chemical potential and finite quark masses perturbative calculations provide results consistent with lattice QCD for temperature larger than about 0.2 GeV [46, 47]. The same technique has been used to compute the EoS at finite chemical potential and vanishing temperature with the very interesting result that the strange quark matter EoS could be stiff enough to support stars with  $2.75M_\odot$  [46]. Here, we adopt the parametrization of the pQCD calculations at finite chemical potential presented

in [47]. This parametrization has only one free parameter, the scale parameter  $X$ , which is the ratio between the renormalization scale and the baryon chemical potential and it ranges between 1 and 4. We choose here the value  $X = 3.5$  for which the maximum mass of quark stars is of  $2.53M_\odot$  (see solid red line in Fig.7).

### 3 Masses and radii: theory vs observations

Let us discuss the information on the mass-radius relation obtained by means of astrophysical observations. The direct and precise measurements of the masses of PSR J1614-2230 with  $M = 1.97 \pm 0.04M_\odot$  [2] and of PSR J0348+0432, with  $M = 2.01 \pm 0.04M_\odot$  [3], clearly represent the most important constraints that theoretical calculations must fulfill. A possible candidate with a mass even larger already exists: it is the black widow pulsar PSR B1957+20 whose mass could be of  $2.4 \pm 0.12M_\odot$  provided that the modeling of the light curves is correct [48]. Taking into account the systematic uncertainties on the light curves fit, the lowest limit for its mass turns out to be of  $1.66M_\odot$ . Other hints for the existence of compact stars heavier than  $2M_\odot$  have been obtained also from the observation and the modeling of short-gamma-ray bursts (GRB). The SWIFT experiment has detected tens of short-GRB whose light curves display extended emissions, X-ray flares and internal plateaux with rapid decay at the end of the plateaux (see [49] and Refs. therein). These observations favor a model for the inner engine of these events which is based on a rapidly spinning millisecond magnetar formed from the merger of two neutron stars. Interestingly, the same stellar objects, but formed after a supernova, could be the inner engine of long GRBs [50] (see paper 2). In [51,49], the detailed modeling of the plateaux seen in short GRBs has provided an important constraint on the maximum mass of compact stars:  $M = 2.46_{-0.15}^{+0.13}M_\odot$  (displayed in Fig. 7). Although this limit is not obtained via a direct mass measurement, it represents a strong indication that the maximum mass of compact stars is significantly larger than  $2M_\odot$ .

Let us discuss now radii measurements. One has to remark that radii measurements are much more uncertain than mass measurements and all the observational constraints are based on specific assumptions made for modeling the spectra of the X-ray emissions. In Refs. [52,53] the fits on the thermal emission of 6 quiescent low-mass X-ray binaries, under the assumption that all of them have the same radius  $R$ , provide the constraint  $R = 9.4 \pm 1.2$  km. We remark however that these results are under debate, see Refs. [54,55]. Other indications of the existence of stars with small radii can be found from the analysis of X-ray bursts in Refs.[56,57]. In particular, at  $1\sigma$ , the analysis of [56] indicates radii of about  $9.5 \pm 1.5$ km and masses of about  $M = 1.6 \pm 0.2M_\odot$  (a previous analysis of 4U1820-30 presented in Ref.[58] has also found rather small radii:  $R = 11.2_{-0.5}^{+0.4}$ km and  $M = 1.29_{-0.07}^{+0.19}M_\odot$ ). For Cyg X-2 a radius of about  $9 \pm 0.5$ km is inferred for the canonical mass of  $1.44 \pm 0.06M_\odot$  [57] while for 4U 1728-34 the suggested ranges are  $8.7 - 9.7$  km for radius and

$1.2 - 1.6M_{\odot}$  for the mass [59]. Also, in the analysis of the X-ray pulsations of SAX J1808.4-3658, at  $3\sigma$  level one obtains that the largest mass star allowed has a radius of 10.6 km and a mass of  $1.4M_{\odot}$ ; the largest radius star has a radius of 12.1 km and a mass of  $1.2M_{\odot}$  [60]. These data and the mass-radius relation of hadronic stars (with deltas and hyperons) are displayed in Fig.8.

On the other hand, significantly larger radii are obtained by means of pulse phase-resolved X-ray spectroscopy of PSR J0437-4715 [61]: the radius is constrained to be larger than  $\sim 14$  km at  $1\sigma$  confidence level assuming the mass of the star to be of  $1.76M_{\odot}$  (this value has been obtained via the radio timing technique in [62]). Similarly, in Ref. [63], a radius larger than about 14 km is obtained for the system RX J1856.53754 by assuming a mass between 1.5 and  $1.8M_{\odot}$ .

The existence of very massive compact stars and the possibility that some neutron stars are very compact represents a serious problem for the theoretical modeling of the EoS of strongly interacting matter. While massive compact stars imply that the EoS is stiff, a soft EoS is instead needed to obtain small radii. This tension is relieved, as proposed in [9], if one assumes that there are two families of coexisting compact stars: hadronic stars which can be very compact and quark stars which can be very massive. Specifically, the massive PSR J1614-2230 and PSR J0348+0432, are interpreted in our scenario as quark stars. Similarly, stars with large radii, as the ones inferred in the analysis of Refs. [61,63], are again interpreted as quark stars. On the other hand, the compact stellar objects such as the ones discussed in the analysis of [52,53,56,57,58,59,60] would be instead hadronic stars.

In Fig. 7 and 8 we display the observational constraints discussed above and three examples of theoretical mass-radius relations (solid and dashed lines) based on the SFHo model with  $\Delta$  and  $\Delta$  and hyperons for the hadronic EoS (here  $x_{\sigma\Delta} = 1.15$ ) and the parametrization presented in [47] for the quark matter EoS. All the constraints are fulfilled if one assumes that hadronic stars and quark stars coexist. Notice that hadronic stars cannot reach masses larger than about  $1.5 - 1.6M_{\odot}$  as a result of the softening caused by the formation of deltas and hyperons. The so called hyperon puzzle, and similarly the delta puzzle pointed out in [37], is easily solved in our two families scenario: hyperons and deltas do reduce the maximum mass of compact stars to values significantly smaller than  $2M_{\odot}$  but this fact does not represent a puzzle since the most massive objects are actually quark stars. Notice that also in the scenarios i) and ii) discussed in the introduction, massive stars are composed mostly of quark matter.

A natural question concerns the way the quark star branch is populated. The stellar configuration for which the solid black line starts to deviate from the solid green line corresponds to the onset of hyperons. Once a critical amount of hyperons is present in the center of the star, nucleation of quark matter can start and can subsequently trigger the conversion to a quark star. The conversion occurs because it is energetically convenient: at a fixed value of the baryonic mass, the gravitational mass of the star

on the quark star branch is smaller than the one on the hadronic star branch (see the brown line for an example of this conversion process). The process of conversion is specifically analyzed in the accompanying paper 2.

## 4 Binary systems

Another useful constraint on the EoS can be obtained also by studying the double pulsar system J0737-3039 [64]. The mass of the so called Pulsar B is of  $1.249 \pm 0.001M_{\odot}$ . Under the assumption that this pulsar formed from an electron capture supernova one can infer a baryonic mass in the range  $1.366 - 1.375M_{\odot}$  [65]. In our scenario we can interpret this star as a hadronic star (which contains  $\Delta$  resonances but which is too light to allow the formation of hyperons). In Fig.9, we display the relation between the gravitational mass and the baryonic mass for hadronic stars and quark stars. In the insert, we show also the constraint of [65]. Our hadronic EoS is perfectly in agreement with the analysis of Ref.[65]: the appearance of delta resonances gives a small additional contribution to the binding energy of hadronic stars as compared to nucleonic stars. When considering only nucleons (see green line), the constraint of [65] is not fulfilled. Notice however that detailed supernova simulations have shown that the uncertainties associated with the EoS and the wind ablation are such that the allowed baryonic mass window is shifted towards smaller values [66].

Low-mass X-ray binaries offer another possible hint for the existence of two families of compact stars. These systems are most probably at the origin of millisecond pulsars: within the so called recycling scenario, the neutron star is spun up to milliseconds periods due to the accretion of mass from its white dwarf companion. Tidal interactions during the accretion phase are responsible for the circularization of the orbit and indeed most of the millisecond pulsars are in circular orbits (with eccentricity  $e$  from  $10^{-7}$  to  $10^{-3}$ ). However, recently, few examples have been discovered having a much larger eccentricity such as PSR J2234+06 for which  $e = 0.13$  (see other examples in [67]). In this system the white dwarf has a mass of  $0.23M_{\odot}$ . The existence of systems with high eccentricities represents a puzzle in the recycling model of pulsars. A possible explanation is that the accreting object, at some point during its evolution, collapses to a more stable configuration thus increasing abruptly the eccentricity of the binary. In Ref. [68] it has been investigated the scenario of a rotationally-delayed accretion- induced collapse of a super-Chandrasekhar mass white dwarf. In Ref.[69] instead, the accreting star is a neutron star which, due to mass accretion, converts into a quark star. In our two families scenario the conversion of a hadronic star to a quark star is necessary once a sufficient amount of strangeness is formed at the center of the star. As one can see in Fig.7, the conversion would occur for masses of the hadronic star between  $\sim 1.35 - 1.6M_{\odot}$  with an energy released in the conversion given by the difference between the gravitational mass of the hadronic star  $M_H$  and the gravitational mass of the quark star  $M_Q$  computed at the same fixed

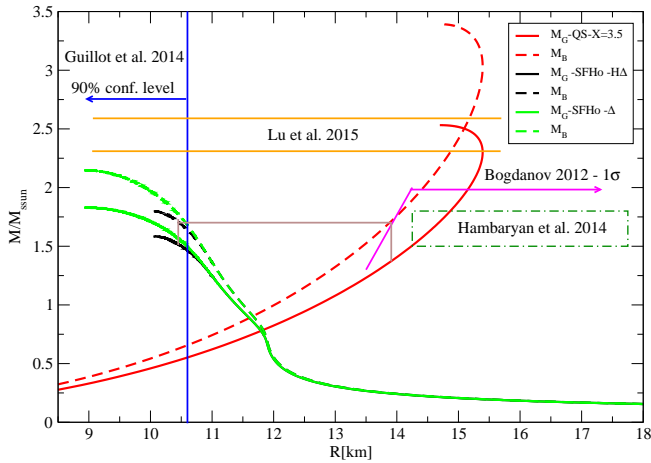


**Fig. 7.** Gravitational mass-radius (solid lines) and baryonic mass-radius (dashed lines) relations for hadronic stars (including only deltas and hyperons and deltas) and quark stars. Some of the most recent observational constraints are also displayed (see text). The brown lines show that given a hadronic star configuration (in which also hyperons are present), the quark star with the same baryon mass has a smaller gravitational mass even if its radius is larger. The conversion of the hadronic star into a quark star would be therefore energetically favored.

baryonic mass:  $\Delta M = M_H - M_Q \sim 0.15M_\odot$  (see Fig. 9). The eccentricity is related to the masses of the hadronic star, of the quark star and of the white dwarf companion  $M_{WD}$  by the following relation:  $e = \Delta M / (M_Q + M_{WD})$ . It results that  $e \sim 0.1$  if one takes  $M_{WD} = 0.23M_\odot$ ,  $M_H = 1.55M_\odot$ ,  $M_Q = 1.4M_\odot$ . A correction to the eccentricity of the order of  $\pm 0.03$  is obtained when considering that during the conversion the newly born stellar object could get a small kick velocity  $v_k$  of the order of 1km/sec [68]. These simple estimates show that in our model the values of the eccentricities are quite close to the measured ones. It would be therefore interesting to investigate more in detail this problem. Future measurements of the masses of the compact stars in those eccentric systems will be crucial to test our scenario.

## 5 Discussion and conclusions

We have discussed several hints of the existence of two coexisting families of compact stars, hadronic stars and quark stars. A first important and widely discussed argument in favor of this scenario is the necessary appearance of delta resonances and hyperons as the central density of a hadronic star reaches values larger than about  $2n_0$ . The formation of these particles softens the EoS and reduces the maximum mass with respect to stars made only of nucleons. How much the maximum mass is reduced due to the appearance of these particles is the subject of a lively and on going research activity in nuclear physics. One one

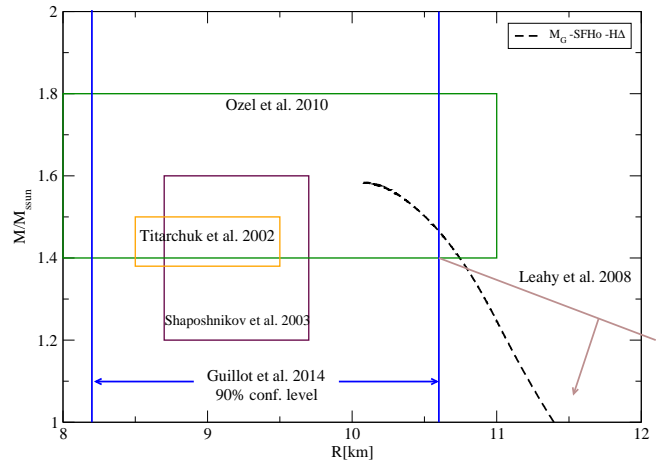


**Fig. 8.** Mass-radius relation for hadronic stars and observational constraints indicating the existence of very compact stellar objects.

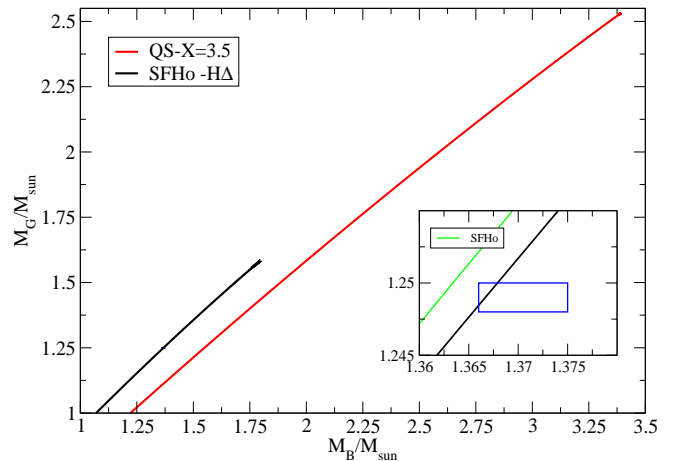


**Fig. 9.** Relation between gravitational mass and baryonic mass for hadronic stars and quark stars. At fixed baryonic mass the difference between the gravitational mass of a hadronic star and a quark star is of the order of  $0.15M_\odot$ . In the insert we display also the curve corresponding to nucleonic stars within the SFHo EoS (green line). The slightly larger binding energy obtained when adding deltas and hyperons allow to fulfill the constraint of [65] (blue box).

hand, in phenomenological calculations based on relativistic mean field models the maximum mass of hyperon stars could still reach the  $2M_\odot$  limit (see for instance [70, 71, 72]) on the other hand in more realistic calculations based on microscopic nucleon-nucleon interactions, the appearance of hyperons is accompanied by a strong softening of the EoS which leads to maximum masses much below  $2M_\odot$  and in some case even below  $1.4M_\odot$  [73, 74, 75]. A possible way out is that the hadronic EoS is so stiff that even for the  $2M_\odot$  star the central density is below the threshold for



the appearance of hyperons: a possible example has been given in [76] where at a mass  $2.09M_{\odot}$  the central density is of  $3.5n_0$  and hyperons are not yet formed. This scenario is realized if the three-body hyperon- nucleon interaction is sufficiently repulsive. Another possible way to add repulsion between baryons is the multi-Pomeron exchange potential proposed in [77] which, again, would allow the existence of massive hadronic stars. Unfortunately from the theoretical side one cannot draw a firm conclusion on the composition of the  $2M_{\odot}$  stars.

The crucial quantity to measure is clearly the radius of compact stars. As already discussed, the presently available analysis are still affected by large systematic errors. While there are some hints in favor of the two families scenario (some analysis suggesting the existence of stars with radii of the order of 10km and some other analysis which infer radii of about 14km) one cannot yet claim that these measurements have found compelling evidence for the two families scenario. However, the Neutron star Interior Composition Explorer (NICER) instrument, to be launched in 2016, will allow to achieve 5% precision in neutron-star radius through rotation-resolved spectroscopy (see for instance [78]). Still another possibility is based on the future X-ray mission ATHENA+ which, combined with accurate distance measurements provided by the GAIA experiment, will also allow to obtain information on masses and radii. Another possible way of extracting the radii is by analyzing the gravitational-wave emission during the merger of two compact stars. In particular, the frequency of the dominant oscillation mode of the post-merger remnant is directly related to the radius of the non-rotating compact star [79]. Again the expected error is of the order of a few hundred meters. With such a precision one would possibly finally establish what the internal composition of compact stars is. Let us consider the canonical  $1.4M_{\odot}$ ; one can imagine three possible outcomes for the measurement of its radius: i) radius larger than about 13.5 km; ii) radius between 11.5 and 13.5 km; iii) radius smaller than about 11.5km. These numbers are also suggested by the model-independent study of Ref.[7].

In the first case, the large radius implies that the EoS is stiff. Therefore the central density of the  $1.4M_{\odot}$  star is small and it is possible that even for the most massive stars the central density is smaller than the threshold of formation of hyperons and deltas. Only “normal” neutron stars would exist. In the second case, the interpretation would be much more complicated: several equations of state have been proposed which can reach the  $2M_{\odot}$  limit and predict a radius of about 12km for the canonical neutron star mass. Hybrid stars and hyperonic stars would be both possible (in particular the scenario i) discussed in the introduction would be favored). In the last case, the only available possibility is the two families scenario that we are here proposing. Indeed there are no examples of equations of state in the literature that can at the same time fulfill the  $2M_{\odot}$  and predict such small radii for the canonical neutron star <sup>1</sup>. Within a few years one could

then expect the NICER experiment to give a final answer to the question about the existence of the two families.

The scenario of two families of compact stars is based on the existence of quark stars together with hadronic stars. In turn the existence of quark stars implies that the Bodmer-Witten hypothesis is correct and therefore also small nuggets of quark matter, the so called strangelets, must exist. We know very little about strangelets: they are expected to be positively charged and to have a very small charge to mass ratio, see [81]. Their mass spectrum is instead completely unknown. As a matter of fact, to date, there is no experimental evidence of the existence of strangelets. A possible way to produce strangelets on earth is through heavy ions experiments: the search for strangelets at RHIC has produced upper limits of few  $10^{-6}$  to  $10^{-7}$  per central Au+Au collision for strangelets with mass larger than 30 GeV [82]. Notice however that the production of strangelets in heavy ions collision requires a net baryon excess [83] which is unlikely to be obtained at RHIC energies. In the context of cosmology a very interesting hypothesis is that strangelets could represent a type of “macro dark matter” which would have been produced by some post-inflationary process [84]. In this scenario, no “beyond standard model physics” would be required to explain the existence of baryonic dark matter. In astrophysics, strangelets could represent an important component of cosmic rays. The events that would most probably produce strangelets are the merger of compact stars with at least one of the two stars being a quark star, see [85] for a discussion on the fragmentation of quark matter into strangelets. The search for strangelets in the lunar soil has provided no evidence of them from A=42 to A=70 and for nuclear charges of 5, 6, 8, 9 and 11 [86]. New limits on the mass and the flux of cosmic strangelets are expected to be available in the near future thanks to the AMS-02 experiment.

From the theoretical side, to date, there has been only one detailed simulation of the merger of two quark stars [87] while the possibility of neutron star - quark star and black hole - quark star merger have not yet been considered. An unexpected result of these simulations is that in many cases, after the merger, a prompt collapse to a black hole occurs and basically no quark matter is ejected. In particular, this occurs for values of the total mass of the merger larger than about  $2.5 - 3M_{\odot}$ . In our scenario quark stars have masses larger than about  $1.35M_{\odot}$  and it is rather difficult to avoid a prompt collapse. It is therefore possible that even if quark matter is absolutely stable the flux of strangelets is vanishingly small and not all compact stars convert into quark stars as it would result if the cosmic strangelets pollution would be significant [88]. The two families of compact stars could indeed coexist.

---

and, at the same time, predict the existence of very compact stars. There are two problems associated with such equations of state and in particular with WFF1[80]: already for the canonical mass the central density is of about  $4n_0$ . At such densities heavy baryons should be included while in WFF1 they are simply neglected. Second: at densities of about  $1\text{fm}^{-3}$  it violates causality.

<sup>1</sup> In Ref. [52], some examples of non-relativistic microscopic calculations of nucleonic matter are shown that fulfill the  $2M_{\odot}$

A.D. would like to thank V. Hislop for the moral support during the preparation of the paper. G.P. acknowledges financial support from the Italian Ministry of Research through the program Rita Levi Montalcini .

## References

1. J. Adams et al. (STAR), Nucl. Phys. **A757**, 102 (2005), [nucl-ex/0501009](#)
2. P. Demorest, T. Pennucci, S. Ransom, M. Roberts, J. Hessels, Nature **467**, 1081 (2010)
3. J. Antoniadis, P.C. Freire, N. Wex, T.M. Tauris, R.S. Lynch et al., Science **340**, 6131 (2013)
4. H. Chen, M. Baldo, G.F. Burgio, H.J. Schulze, Phys. Rev. **D84**, 105023 (2011), [1107.2497](#)
5. L. Bonanno, A. Sedrakian, Astron. Astrophys. **539**, A16 (2012), [1108.0559](#)
6. J.L. Zdunik, P. Haensel, Astron. Astrophys. **551**, A61 (2013), [1211.1231](#)
7. A. Kurkela, E.S. Fraga, J. Schaffner-Bielich, A. Vuorinen, Astrophys. J. **789**, 127 (2014), [1402.6618](#)
8. S. Benic, D. Blaschke, D.E. Alvarez-Castillo, T. Fischer, S. Typel, Astron. Astrophys. **577**, A40 (2015), [1411.2856](#)
9. A. Drago, A. Lavagno, G. Pagliara, Phys.Rev. **D89**, 043014 (2014), [1309.7263](#)
10. N. Glendenning, S. Moszkowski, Phys.Rev.Lett. **67**, 2414 (1991)
11. J.M. Lattimer, Y. Lim, ApJ. 771, **51** (2013), [1203.4286](#)
12. A.W. Steiner, M. Prakash, J.M. Lattimer, P.J. Ellis, Phys.Rept. **411**, 325 (2005), [nucl-th/0410066](#)
13. A.W. Steiner, M. Hempel, T. Fischer, Astrophys.J. **774**, 17 (2013), [1207.2184](#)
14. A.R. Raduta, F. Gulminelli, M. Oertel (2014), [1406.0395](#)
15. J. Schaffner, C.B. Dover, A. Gal, C. Greiner, H. Stoecker, Phys.Rev.Lett. **71**, 1328 (1993)
16. J. Schaffner, I.N. Mishustin, Phys.Rev. **C53**, 1416 (1996)
17. E.E. Zabrodin, I.C. Arsene, J. Bleibel, M. Bleicher, L.V. Bravina et al., J.Phys. **G36**, 064065 (2009)
18. M. Hofmann, R. Mattiello, H. Sorge, H. Stoecker, W. Greiner, Phys.Rev. **C51**, 2095 (1995)
19. S. Bass, M. Gyulassy, H. Stoecker, W. Greiner, J.Phys. **G25**, R1 (1999)
20. A. Lavagno, Phys.Rev. **C81**, 044909 (2010)
21. A. Lavagno, D. Pigato, Phys.Rev. **C86**, 024917 (2012)
22. H. Huber, F. Weber, M. Weigel, C. Schaab, Int.J.Mod.Phys. **E7**, 301 (1998), [nucl-th/9711025](#)
23. H. Xiang, G. Hua, Phys.Rev. **C67**, 038801 (2003)
24. Y. Chen, H. Guo, Y. Liu, Phys.Rev. **C75**, 035806 (2007)
25. Y. Chen, Y. Yuan, Y. Liu, Phys.Rev. **C79**, 055802 (2009)
26. T. Schurhoff, S. Schramm, V. Dexheimer, Astrophys.J. **724**, L74 (2010)
27. N. Glendenning, Astrophys.J. **293**, 470 (1985)
28. D. Kosov, C. Fuchs, B. Martemyanov, A. Faessler, Phys.Lett. **B421**, 37 (1998)
29. X.m. Jin, Phys.Rev. **C51**, 2260 (1995)
30. E. Oset, L. Salcedo, Nucl.Phys. **A468**, 631 (1987)
31. J. Koch, N. Ohtsuka, Nucl.Phys. **A435**, 765 (1985)
32. K. Wehrberger, C. Bedau, F. Beck, Nucl.Phys. **A504**, 797 (1989)
33. J. O'Connell, R. Sealock, Phys.Rev. **C42**, 2290 (1990)
34. W. Alberico, G. Gervino, A. Lavagno, Phys.Lett. **B321**, 177 (1994)
35. Y. Horikawa, M. Thies, F. Lenz, Nucl.Phys. **A345**, 386 (1980)
36. S. Nakamura, T. Sato, T.S. Lee, B. Szczerbinska, K. Kubodera, Phys.Rev. **C81**, 035502 (2010), [0910.1057](#)
37. A. Drago, A. Lavagno, G. Pagliara, D. Pigato, Phys. Rev. **C90**, 065809 (2014), [1407.2843](#)
38. B.J. Cai, F.J. Fattoyev, B.A. Li, W.G. Newton, Phys. Rev. **C 92**, 015802 (2015)
39. B.A. Li (2015), [1507.03279](#)
40. J. Benlliure et al., JPS Conf. Proc. **6**, 020039 (2015)
41. Z.X. Li, G.J. Mao, Y.Z. Zhuo, W. Greiner, Phys.Rev. **C56**, 1570 (1997)
42. S. Typel, G. Ropke, T. Klahn, D. Blaschke, H. Wolter, Phys.Rev. **C81**, 015803 (2010), [0908.2344](#)
43. B.J. Cai, F.J. Fattoyev, B.A. Li, W.G. Newton, Phys. Rev. **C92**, 015802 (2015), [1501.01680](#)
44. M. Prakash, I. Bombaci, M. Prakash, P.J. Ellis, J.M. Lattimer, R. Knorren, Phys. Rept. **280**, 1 (1997), [nucl-th/9603042](#)
45. M. Buballa, Phys. Rept. **407**, 205 (2005), [hep-ph/0402234](#)
46. A. Kurkela, P. Romatschke, A. Vuorinen, Phys.Rev. **D81**, 105021 (2010), [0912.1856](#)
47. E.S. Fraga, A. Kurkela, A. Vuorinen, Astrophys.J. **781**, L25 (2014), [1311.5154](#)
48. M. van Kerkwijk, R. Breton, S. Kulkarni, Astrophys.J. **728**, 95 (2011)
49. H.J. L, B. Zhang, W.H. Lei, Y. Li, P.D. Lasky, Astrophys.J. **805**, 89 (2015), [1501.02589](#)
50. B. Metzger, D. Giannios, T. Thompson, N. Bucciantini, E. Quataert (2010)
51. P.D. Lasky, B. Haskell, V. Ravi, E.J. Howell, D.M. Coward, Phys.Rev. **D89**, 047302 (2014), [1311.1352](#)
52. S. Guillot, M. Servillat, N.A. Webb, R.E. Rutledge (2013), [1302.0023](#)
53. S. Guillot, R.E. Rutledge, Astrophys.J. **796**, L3 (2014), [1409.4306](#)
54. J.M. Lattimer, A.W. Steiner (2013), [1305.3242](#)
55. C.O. Heinke et al., Mon. Not. Roy. Astron. Soc. **444**, 443 (2014), [1406.1497](#)
56. F. Ozel, G. Baym, T. Guver, Phys.Rev. **D82**, 101301 (2010), [1002.3153](#)
57. L. Titarchuk, N. Shaposhnikov, Astrophys. J. **570**, L25 (2002), [astro-ph/0203432](#)
58. N. Shaposhnikov, L. Titarchuk, Astrophys. J. **606**, L57 (2004), [astro-ph/0403488](#)
59. N. Shaposhnikov, L. Titarchuk, F. Haberl, Astrophys. J. **593**, L35 (2003), [astro-ph/0307215](#)
60. D.A. Leahy, S.M. Morsink, C. Cadeau, Astrophys. J. **672**, 1119 (2008), [astro-ph/0703287](#)
61. S. Bogdanov, Astrophys.J. **762**, 96 (2013), [1211.6113](#)
62. J.P.W. Verbiest, M. Bailes, W. van Straten, G.B. Hobbs, R.T. Edwards, R.N. Manchester, N.D.R. Bhat, J.M. Sarkissian, B.A. Jacoby, S.R. Kulkarni, Astrophys. J. **679**, 675 (2008), [0801.2589](#)
63. V. Hambaryan, R. Neuhaeuser, V. Suleimanov, K. Werner, Journal of Physics: Conf.Ser. **496**, 012015 (2014)
64. M. Burgay et al., Nature **426**, 531 (2003), [astro-ph/0312071](#)
65. P. Podsiadlowski, J.D.M. Dewi, P. Lesaffre, J.C. Miller, W.G. Newton, J.R. Stone, Mon. Not. Roy. Astron. Soc. **361**, 1243 (2005), [astro-ph/0506566](#)
66. F.S. Kitaura, H.T. Janka, W. Hillebrandt, Astron. Astrophys. **450**, 345 (2006), [astro-ph/0512065](#)

67. B. Knispel et al., *Astrophys. J.* **806**, 140 (2015), 1504.03684
68. P.C.C. Freire, T.M. Tauris, *Mon.Not.Roy.Astron.Soc.* **438**, 86 (2014), 1311.3478
69. L. Jiang, X.D. Li, J. Dey, M. Dey, *Astrophys.J.* **807**, 41 (2015), 1505.04644
70. S. Weissenborn, D. Chatterjee, J. Schaffner-Bielich, *Phys.Rev.* **C85**, 065802 (2012)
71. S. Weissenborn, D. Chatterjee, J. Schaffner-Bielich, *Nucl.Phys.* **A881**, 62 (2012), 1111.6049
72. I. Bednarek, P. Haensel, J. Zdunik, M. Bejger, R. Manka (2011), 1111.6942
73. M. Baldo, G. Burgio, H. Schulze, *Phys.Rev.* **C61**, 055801 (2000), nucl-th/9912066
74. I. Vidana, D. Logoteta, C. Providencia, A. Polls, I. Bombaci, *Europhys.Lett.* **94**, 11002 (2011), 1006.5660
75. H. Djapo, B.J. Schaefer, J. Wambach, *Phys. Rev.* **C81**, 035803 (2010), 0811.2939
76. D. Lonardoni, A. Lovato, S. Gandolfi, F. Pederiva, *Phys. Rev. Lett.* **114**, 092301 (2015), 1407.4448
77. Y. Yamamoto, T. Furumoto, N. Yasutake, T.A. Rijken, *Phys. Rev.* **C90**, 045805 (2014), 1406.4332
78. D. Psaltis, F. zel, D. Chakrabarty, *Astrophys. J.* **787**, 136 (2014), 1311.1571
79. A. Bauswein, N. Stergioulas, H.T. Janka (2015), 1508.05493
80. R.B. Wiringa, V. Fiks, A. Fabrocini, *Phys.Rev.* **C38**, 1010 (1988)
81. J. Madsen, *Phys.Rev.* **D71**, 014026 (2005), astro-ph/0411538
82. B.I. Abelev et al. (STAR), *Phys. Rev.* **C76**, 011901 (2007), nucl-ex/0511047
83. C. Greiner, P. Koch, H. Stoecker, *Phys. Rev. Lett.* **58**, 1825 (1987)
84. D.M. Jacobs, G.D. Starkman, B.W. Lynn, *Mon. Not. Roy. Astron. Soc.* (2014), 1410.2236
85. L. Paulucci, J.E. Horvath, *Phys. Lett.* **B733**, 164 (2014), 1405.1777
86. K. Han, J. Ashenfelter, A. Chikanian, W. Emmet, L.E. Finch, A. Heinz, J. Madsen, R.D. Majka, B. Monreal, J. Sandweiss, *Phys. Rev. Lett.* **103**, 092302 (2009), 0903.5055
87. A. Bauswein, H.T. Janka, R. Oechslin, G. Pagliara, I. Sagert et al., *Phys.Rev.Lett.* **103**, 011101 (2009)
88. J.L. Friedman, R.R. Caldwell, *Phys. Lett.* **B264**, 143 (1991)